

Investigation of absorption coefficient measurement of acoustical materials by boundary element method using particle velocity and sound pressure sensor in free field

Kunikazu Hirosawa*, Hiroshi Nakagawa, Makoto Kon and Aki Yamamoto

Nittobo Acoustic Engineering Co., Ltd.

(Received 30 March 2009, Accepted for publication 13 May 2009)

Keywords: Absorption coefficient, Free field, Area effect, Spherical wave field, Boundary element method

PACS number: 43.58.Bh, 43.20.Rz [doi:10.1250/ast.30.442]

1. Introduction

There are many methods of measuring the absorption coefficient or the acoustic impedance of acoustical materials. For the normal incident absorption coefficient and acoustic impedance measurement, the method using the impedance tube [1] may be used. In this method, however, the dimensions of the impedance tube limit the frequency range in which the value can be properly measured, and also, the specimen must be cut out from a large material block. Moreover, the measured results of the large material block itself and of the small cut specimen tend to differ when the specimen is a poroelastic material.

The authors focus on the measurement method using the particle velocity and sound pressure sensor (PU-Probe) [2] in a free field. The method can be used to measure the essential properties of a material regardless of the specimen size. Therefore, it could overcome the above mentioned problem. In this paper, the effects of receiver positions and specimen areas are discussed as a part of our study on the measurement of the absorption coefficient in a free field. In order to eliminate noise from the measuring system and unwanted reflected waves, the boundary element method (BEM) is applied in these investigations.

2. Analysis model

Figure 1 shows a three-dimensional hemi-free field with an infinite and rigid x - y plane. The absorbing area F that consists of $L[\text{m}] \times L[\text{m}]$ is fixed on the x - y plane and the origin of the orthogonal coordinate system is at the center of F . The receiver R or the PU-Probe is located at height h_R from the x - y plane. The incident angle between the line from the real sound source S to the intersection point R_0 and the z -axis is θ , and the distance is $r[\text{m}]$.

2.1. Boundary element method

By applying the mirror image method, the analysis model becomes equivalent to the situation that F of thickness 0 floats on the x - y plane in a free field and the real sound source S and the imaginary sound source S' , which are symmetrical to the x - y plane, exist. F is assumed to be a locally reacting surface with the normal specific acoustic impedance Z_n of 25 mm glass wool (flow resistivity 55,000 Ns/m⁴). Z_n is estimated using the empirical equation proposed by Allard and Champoux [3].

In this study, the sound field is calculated by the BEM applying the mirror image method for the sound pressure and the particle velocity [4]. The boundary element is the quadrilateral constant element, and the maximum element length is less than 1/8 wavelength at each frequency. The formulation of the BEM in the frequency domain considers the whole edge effect.

2.2. Surface impedance method

Figure 2 shows the situation that the sound is incident upon F with angle θ . r_r is the distance between S and R , and r_i is the distance between S' and R . θ_r is the angle between r_r and the z -axis, and θ_i is the angle between r_i and the z -axis. Distances r_r and r_i are assumed to be sufficiently long compared with the wavelength, and F is assumed to be the locally reacting surface shown in Fig. 2.

The ratio of the sound pressure $p(R)$ and the $-z$ directional particle velocity $u_n(R)$, which are obtained by the BEM, is expressed as $Z_n(R)$. For a plane wave with incident angle θ , the sound pressure reflection coefficient $R_p(\theta)$ is given by [5]

$$R_p(\theta) = \frac{\frac{e^{-jkr_r}}{r_r} Z_n(R) \frac{1 + jkr_r}{jkr_r} \cos \theta_r - \rho c}{\frac{e^{-jkr_i}}{r_i} Z_n(R) \frac{1 + jkr_i}{jkr_i} \cos \theta_i + \rho c}. \quad (1)$$

3. Effect of receiver positions

To investigate the effect of receiver position on the absorption coefficient, the sound pressure and the particle velocity at four receiver points, $R_1 = (0, 0, 0.01)$, $R_2 = (0.1, 0, 0.01)$, $R_3 = (0.1, 0.1, 0.01)$, and $R_4 = (0.1, 0.05, 0.01)$, are calculated by the BEM. Distance r is fixed at 1.0 m, the incident angles are $\theta = 0^\circ, 60^\circ$ ($\varphi = 0^\circ$), and the absorbing area is 1.0 m \times 1.0 m.

Figure 3 shows the absorption coefficient α_0 at four receiver points for normal incidence, and Fig. 4 shows the absorption coefficient α_{60} at the same points for $\theta = 60^\circ$ incidence.

From these figures, differences in α_0 caused by different receiver positions are seen, however, the values of α_{60} are not affected by the change in receiver position. With normal incidence, in particular, R_1 is the center of the specimen and the diffracted waves from all edges of the specimen equally affect the result occurring at R_1 . It can also cause the

*e-mail: hirosawa@noe.co.jp

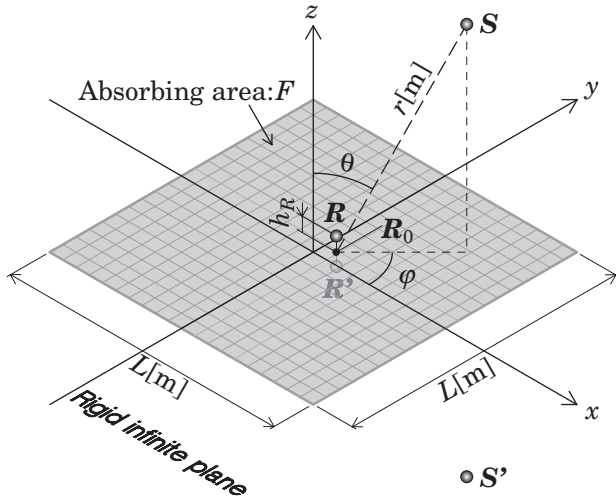


Fig. 1 Analysis model. S : Real source; S' : Imaginary source; R : Real receiver; R' : Imaginary receiver; h_R : Receiver height; R_0 : Intersection point of the perpendicular made from R to F .

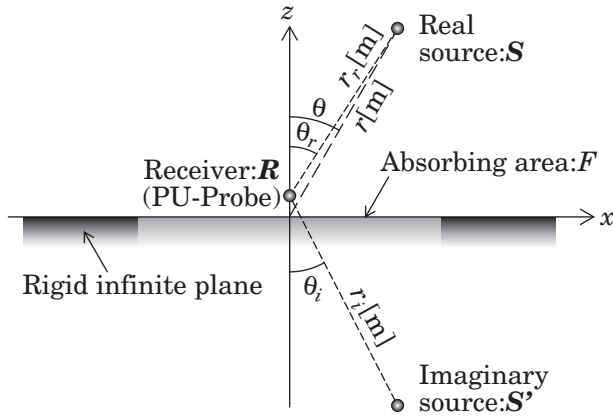


Fig. 2 Illustration of surface impedance method.

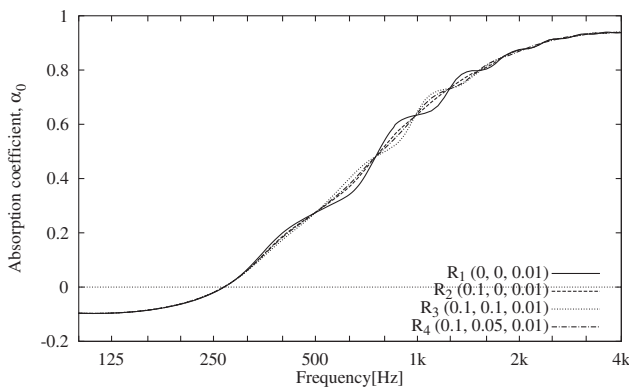


Fig. 3 α_0 at various receiver positions. $r = 1.0$ m, specimen area is $1.0 \text{ m} \times 1.0 \text{ m}$.

deviation of α_0 . In contrast, the effect of the diffracted waves at R_4 is dispersed as a result of the different distances between each edge and R_4 . Furthermore, Fig. 3 also indicates that the

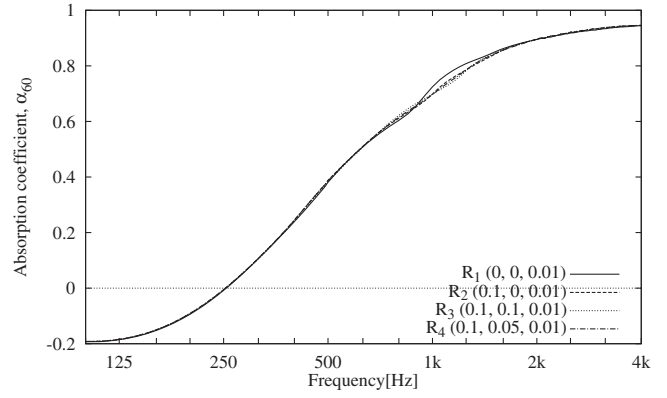


Fig. 4 α_{60} at various receiver positions. $r = 1.0$ m, specimen area is $1.0 \text{ m} \times 1.0 \text{ m}$.

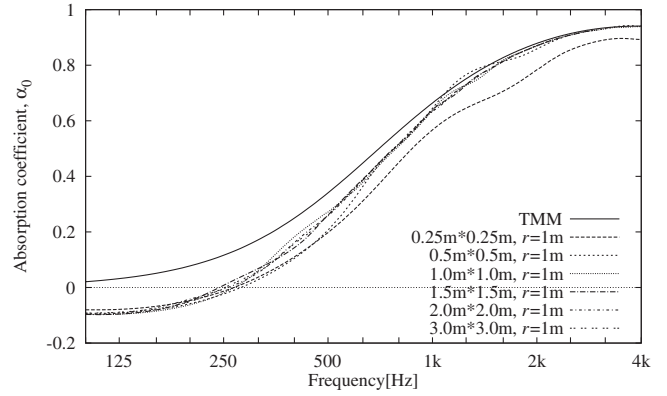


Fig. 5 α_0 for various specimen areas. $r = 1.0$ m, $\theta = 0^\circ$.

value of α_0 at R_4 is the most stable. Therefore, the receiver position in this measurement should not be the center. According to this discussion, the receiver position for the investigation of the absorption coefficient measured by the surface impedance method is R_4 after this section.

4. Effect of specimen areas

The effect of the specimen area on the absorption coefficient is investigated. The dimensions of the specimen are $0.25 \text{ m} \times 0.25 \text{ m}$, $0.5 \text{ m} \times 0.5 \text{ m}$, $1.0 \text{ m} \times 1.0 \text{ m}$, $1.5 \text{ m} \times 1.5 \text{ m}$, $2.0 \text{ m} \times 2.0 \text{ m}$ and $3.0 \text{ m} \times 3.0 \text{ m}$. The receiver position is $R_4 = (0.1, 0.05, 0.01)$, the distances r are 1.0 m and 2.0 m , and the incident angles are $\theta = 0^\circ$ and 60° ($\varphi = 0^\circ$).

Figure 5 shows the absorption coefficient α_0 for each specimen area with $r = 1.0 \text{ m}$ and $\theta = 0^\circ$. In the same way, Fig. 6 shows α_{60} with $r = 1.0 \text{ m}$ and $\theta = 60^\circ$, Fig. 7 shows α_0 with $r = 2.0 \text{ m}$ and $\theta = 0^\circ$, and Fig. 8 shows α_{60} with $r = 2.0 \text{ m}$ and $\theta = 60^\circ$ ($\varphi = 0^\circ$). The curves marked "TMM" in these figures describe the absorption coefficient calculated by the transfer matrix method (TMM) [6]. The propagation constant and the characteristic impedance in the TMM are also estimated using Allard and Champoux's model [3]. Therefore, the situation assumed in the TMM is that a plane wave propagates into a specimen of infinite area, and the effect of the specimen area is not considered.

It is found that both the normal and $\theta = 60^\circ$ incidences of the absorption coefficient are affected by the specimen areas.

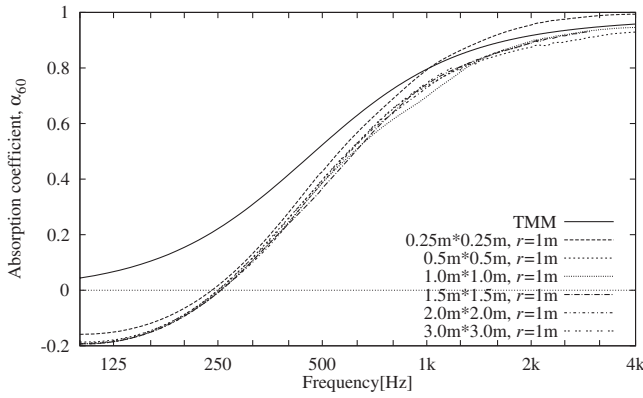


Fig. 6 α_{60} for various specimen areas. $r = 1.0$ m, $\theta = 60^\circ$.

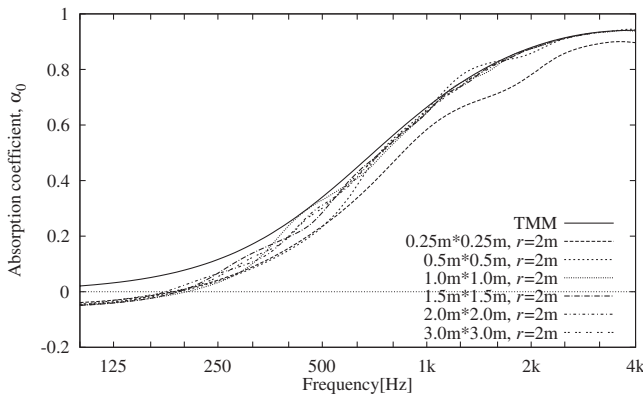


Fig. 7 α_0 for various specimen areas. $r = 2.0$ m, $\theta = 0^\circ$.

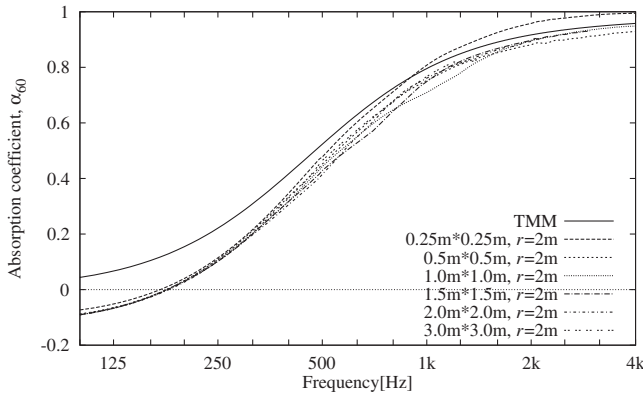


Fig. 8 α_{60} for various specimen areas. $r = 2.0$ m, $\theta = 60^\circ$.

The absorption coefficient with normal incidence tends to converge at the curve when the areas are larger than $1.0\text{ m} \times 1.0\text{ m}$, and one with $\theta = 60^\circ$ incidence tends to converge at the other curve when the areas are larger than $1.5\text{ m} \times 1.5\text{ m}$. However, the convergence values depend on distance r , and are negative values at low frequency.

4.1. Effect of distances between source and receivers

Figure 9 shows the absorption coefficient of distance r with normal incidence, which is calculated using Eq. (1). The impedance $Z_n(\mathbf{R})$ is estimated using Allard and Champoux's model [3] (flow resistivity $55,000\text{ Ns/m}^4$), and the receiver

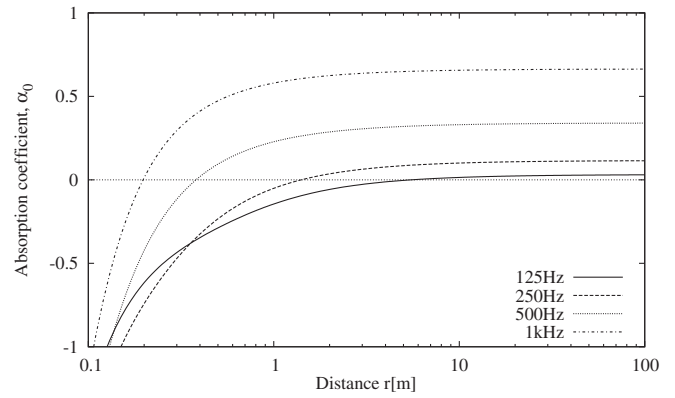


Fig. 9 Distance characteristics of α_0 at 125 Hz, 250 Hz, 500 Hz and 1 kHz.

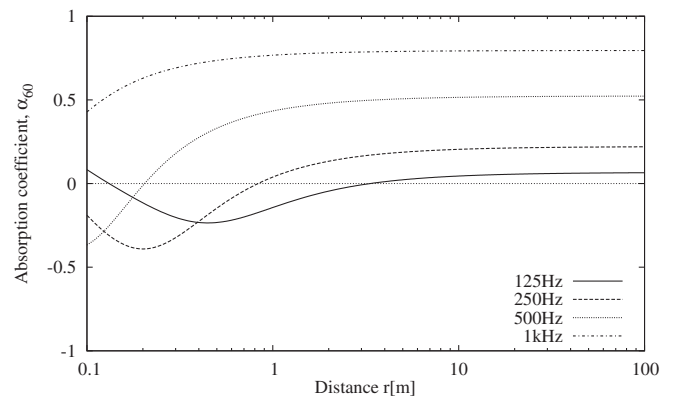


Fig. 10 Distance characteristics of α_{60} at 125 Hz, 250 Hz, 500 Hz and 1 kHz.

height is $h_R = 1\text{ cm}$. Figure 10 shows the absorption coefficient of distance r with $\theta = 60^\circ$ incidence. These figures indicate that the values tend to converge to constant values as r becomes longer, because Eq. (1) describes the plane wave reflection coefficient under the condition of $r \rightarrow \infty$. On the contrary, when r is less than about 10 m, the absorption coefficient becomes lower and a negative value. Therefore, in Figs. 5–8, the major cause of the absorption coefficient becoming negative at low frequency is distance r , not the effect of the specimen area. For this reason, the assumption of plane wave propagation at the neighborhood of the receiver is not correct.

4.2. Comparison with Ingard's exact solution

From the results described in the previous section, when the effect of the specimen area is investigated, the absorption coefficient of an infinite area, which is used as the reference value, must be calculated in the spherical wave field, and the effect of distance r on Eq. (1) must be equal in each area. In this paper, the reference absorption coefficient of an infinite area is taken from Ingard's exact solution that describes the solution above the infinite plane with a finite normal specific acoustic impedance Z_n in the three-dimensional hemi-free field [7].

As Fig. 11 shows, the real source S and the imaginary source S' exist on the z -axis, and the angle between the line

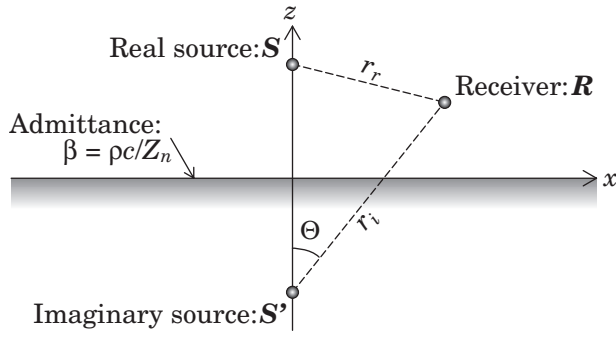


Fig. 11 Geometry of the propagation problem.

from S' to the receiver R and the z -axis is Θ . When the normal specific acoustic admittance ratio normalized by ρc is $\beta = \rho c / Z_n$ and the time-dependent factor is $\exp(-j\omega t)$, the sound pressure $p(R)$ is given as

$$p(R) = \frac{e^{jkr_i}}{r_i} + \frac{e^{jkr_r}}{r_r} \{R_p + (1 - R_p)F\}, \quad (2)$$

$$F = 1 - (\beta + \gamma_0)(kr_i)$$

$$\times \int_0^\infty \frac{e^{-(kr_i)t} dt}{\sqrt{(1 + \beta\gamma_0 + jt)^2 - (1 - \gamma_0^2)(1 - \beta^2)}},$$

$$\gamma_0 = \cos \Theta, \quad R_p = (\gamma_0 - \beta)/(\gamma_0 + \beta),$$

where an infinite plane is assumed to be locally reactive, and the $-z$ directional particle velocity $u_n(R)$ is obtained by the normal derivative of the sound pressure, $u_n(R) = 1/j\omega\rho \cdot (\partial p(R)/\partial n)$.

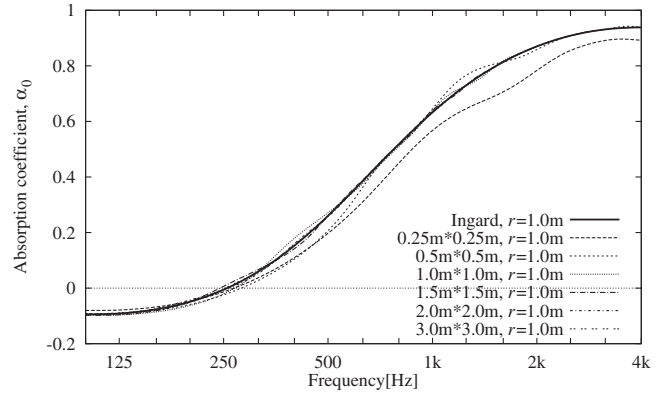
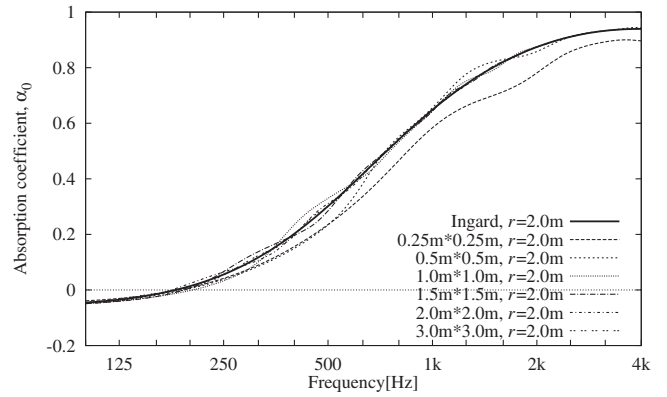
Figure 12 shows the absorption coefficient of each finite specimen area and an infinite area for $r = 1.0$ m, $\theta = 0^\circ$, and Fig. 13 shows the absorption coefficient for $r = 2.0$ m, $\theta = 0^\circ$.

These figures indicate that the absorption coefficient calculated with areas larger than $1.0 \text{ m} \times 1.0 \text{ m}$ approximately coincides with that of an infinite area for normal incidence.

5. Conclusions

In this study, for the locally reactive specimen, the sound field has been calculated by the BEM, and the absorption coefficient has been estimated by the surface impedance method. As a result, following outcomes were obtained.

- Placing the receiver at the center of the specimen should be avoided.
- The measurement of the absorption coefficient by the surface impedance method is affected by the distance between the sound source and the receiver point. For a short distance, the absorption coefficient can be a negative value at low frequency.
- The effect of the specimen area in the surface impedance method is not significant. Although the calculation in this study has been made under the steady state, the effect becomes smaller when the specimen is larger than $1.0 \text{ m} \times 1.0 \text{ m}$.

Fig. 12 α_0 for various specimen areas. $r = 1.0$ m, $\theta = 0^\circ$.Fig. 13 α_0 for various specimen areas. $r = 2.0$ m, $\theta = 0^\circ$.

In further studies, correction of the spherical wave field and a measurement method for obtaining a valid absorption coefficient will be investigated.

References

- [1] JIS A 1405 (2007), ISO 10534 (1998), "Acoustics — Determination of sound absorption coefficient and impedance in impedance tubes — Part 1 and 2."
- [2] H. E. de Bree, "An overview of microflow technologies," *Acta Acustica united with Acustica*, **89**, 163–172 (2003).
- [3] J. F. Allard and Y. Champoux, "New empirical equations for sound propagation in rigid frame fibrous materials," *J. Acoust. Soc. Am.*, **91**, 3346–3353 (1992).
- [4] Y. Kawai, "On the area effect in the reverberation absorption coefficient," *J. Acoust. Soc. Jpn. (J)*, **63**, 268–274 (2007) (in Japanese).
- [5] R. Lanoye, G. Vermeir, W. Lauriks, R. Kruse and V. Mellert, "Measuring the free field acoustic impedance and absorption coefficient of sound absorbing materials with a combined particle velocity-pressure sensor," *J. Acoust. Soc. Am.*, **119**, 2826–2831 (2006).
- [6] B. Brouard, D. Lafarge and J. F. Allard, "A general method of modelling sound propagation in layered media," *J. Sound Vib.*, **183**, 129–142 (1995).
- [7] U. Ingard, "On the reflection of a spherical sound wave from an infinite plane," *J. Acoust. Soc. Am.*, **23**, 329–335 (1951).